



Stress Analysis of Spiral Bevel Gear Drives

Mohammad Qasim Abdullah

University of Baghdad/ College of Engineering
Mechanical Engineering Department

Humam Abdulrahim Abdulwahid

University of Baghdad/ College of Engineering
Mechanical Engineering Department

ABSTRACT

This paper presents numerical and experimental stress analyses to evaluate the contact and bending stresses on the teeth of spiral bevel gear drive. Finite Element Method has been adopted as a numerical technique which accomplished basically by using ANSYS software package. The experimental stress analysis has been achieved by using a gear tooth model made of Castolite material which has photoelastic properties. The main goal of this research is detecting the maximum tooth stresses to avoid the severe areas that caused tooth failure and to increase the working life for this type of gear drives.

Keywords: spiral, bevel, gear, generation, simulation, teeth meshing, stress analysis

الخلاصة

هذا البحث يقدم تحليلاً للاجهادات التي تظهر على المسنن المخروطي الحلزوني عددياً باستخدام تقنيته العناصر المحددة وعملياً باستخدام طريقة التحليل الضوئي للمرونة لايجاد قيم اجهادات التلامس والحناية على سطح السن. الهدف الرئيسي من هذا البحث هو تحديد قيم اجهادات التلامس والحناية القصوى التي يتعرض لها هذا النوع من المسننات لتجنب حدوث الفشل وضمان عمل المسنن لفترة زمنية أطول.

INTRODUCTION

Bevel gear are most suitable widely used in transmission power and motion from the shafts oriented in intersecting axes , therefore the gear have conical pitch surfaces. Spiral bevel gear has a spiral angle and the teeth of such gear drive are curved and oblique and as a result have a considerable amount of overlap. Because of continuous contact the spiral bevel has large load-carrying capacity and run in high speed and more smoothly and quietly than straight bevel gears of the same size. The curved teeth of spiral bevel gear drive ensures more than one tooth in contact at all time and results in gradual engagement and continuous pitch-line contact.

EXPERIMENTAL ANALYSIS

Photoelastic analysis is a widely used technique to perform stress analysis experimentally with a reasonable percent of errors. The present photoelastic study conducted successfully and values of stresses has been determined. Essentially such a problem defined as a three-dimensional problem and it required using a stress-freezing method. Therefore, this study has been reduced to series of two-dimensional problem by calculating the stresses at a number of thin cross sections along the



tooth length ,**M. Q. Abdullah, 1997**. The distribution of contact and bending stresses had been determined.

THE PHOTOELASTICITY METHOD OF STRESS ANALYSIS

Basically we used a transparent material which has a properties leads to simplifying such problems experimentally. One of these properties is transparency to the light which employed in the polariscope. These materials are so called photoelastic materials or birefringent materials ,**Robert F. and George D., 1999**.

The basic equation which calculates experimental stresses is:

$$(\sigma_1 - \sigma_2) = n f / h \quad (1)$$

Where n represent the number of fringes, f is material fringe constant and $(\sigma_1 - \sigma_2)$ is the difference between principal stresses.

PHOTOELASTIC MATERIAL

The used material for models was "Castolite" with (4 mm) thickness such material can be applied for two dimensional studies.

Table 1. shows the material properties that conducted from calibration test of sample which has been taken from same material of sheet used to fabricate the tooth model.

PHOTOELASTIC MODEL

The segment model with one tooth profile has been chosen carefully to matching the output of theoretical design with curved-edged tool of cutting. The gear teeth model was made 7 times actual size. The dimensions of gear geometry of the chosen profile are given in **Table 2**.

EXPERIMENTAL APPARATUS AND CALIBRATION METHOD

In such analysis the stress distribution in a complex model is sought as a function of the load , **Litvin and Alfonso, 2003**.

The accurate calculations of stress distribution need a careful calibration of the material fringe value. These values affected with many parameters such as applied load, temperature and the age of material , **Lelkes and Marialigeti, 2002**.

As an example of the concept of using a calibration specimen that exhibits several fringe orders simultaneously, beam tensile stress is useful and this method used in the present work. An axial load applied on specimen that causes appearance of fringe pattern in the center of the specimen as shown in Fig. (3).

The calculation of the tensile stress for a rectangular specimen of thickness t and width b is:

$$\sigma_1 = \sigma_x = F / dt \quad (2)$$

Referring to eq. (1):

$$F / dt = n f / h \quad (3)$$

Here $t = h$, so

$$f / t = \sigma_1 / n \quad (4)$$

After applying sufficient load F , several orders of fringes appeared. Table (3) shows the results of calibration. Fig.(4) shows the results of photoelastic fringes, gradually increasing the contact and bending stresses for both light and dark field.

EXPERIMENTAL PROCEDURE

The gear teeth model was positioned in the loading fixture such that the point of contact on the gear tooth profile matched the point of contact on the pinion tooth profile. The model of the gear tooth was firmly clamped to prevent rotation and connected to the load sensor which was connected to the load cell to read the load applied, and another gear (pinion) tooth was connected to the arm which connects to the crank handle to apply load by turning the load crank on the loading fixture. Both a light and dark field was employed to increase the accuracy of the account of the fringes in the calibration specimen. Once the load was established, a light field and dark field photograph were taken of the fringe pattern in the gear model. Before conducting any test on the model, the calibration of load cell must be checked. The model is then aligned in the field of the polariscope, and the load is gradually applied to the models. The above procedure is carried out for all the photoelastic models.

TRANSITION FROM MODEL TO PROTOTYPE

For many practical two-dimensional elastic problems with forces applied to external boundaries, stresses depend upon geometry and external forces only. A model must then be geometrically similar to the prototype and the applied loads must be similarly distributed, but they may differ in magnitude by a factor of proportionality. Any stress, σ_{th} in the prototype is determined from the corresponding stress, σ_{exp} at the corresponding point in the model, **Litvin F. L. and Lee H., 1989.**

$$p_{max} = \sigma_{max} = \frac{3}{2} C_p W^{1/3} \left(\frac{B+A}{\phi} \right)^{2/3} (A/B)^{0.186} \quad (5)$$

Where

$$\phi = \frac{1 - \nu_1^2}{E_1} + \frac{1 - \nu_2^2}{E_2}$$

Then

$$\frac{\sigma_{max)_{th}}}{\sigma_{max)_{exp}} = \frac{\frac{3}{2} C_p W_{th}^{1/3} \left(\frac{B+A}{\phi_{th}} \right)^{2/3} (A/B)_{th}^{0.186}}{\frac{3}{2} C_p W_{exp}^{1/3} \left(\frac{B+A}{\phi_{exp}} \right)^{2/3} (A/B)_{exp}^{0.186}} \quad (6)$$

Since the gear teeth models were made 7 times of actual size, thus

$$A, B)_{th} = \frac{1}{7} A, B)_{exp} \quad (7)$$

Where (A) and (B) are the length of major and minor axis of the contact ellipse.

The material is steel with the properties of Young's Modulus $E = 2.068 \times 10^5 \text{ MPa}$ and Poisson's ratio $\nu = 0.29$, and the material properties of photoelastic is shown in Table (1) thus

$$\phi)_{th} = 8.857833 \times 10^{-12} \text{ m}^2 / \text{N} \quad \& \quad \phi)_{exp} = 4.085732 \times 10^{-10} \text{ m}^2 / \text{N}$$

Then

$$\frac{\sigma_{\max})_{th}}{\sigma_{\max})_{exp}} = 47.064519 \left(\frac{W_{th}}{W_{exp}} \right)^{1/3} \quad (8)$$

NUMERICAL ANALYSIS

In accordance with the described procedure for calculation of stresses on tooth flanks, it can be concluded that the solving of the defined task by the analytical methods is very complex and possible only with many assumptions. So, for this problem, as well as for almost all problems in theory of elasticity, the numerical methods must be used. Instead of a system of differential (simple, partial and integral) equations, which are defined for solving some problem in theory of elasticity, numerical methods form corresponding system of simple algebraic equations. By using computers, that system can be solved quickly and successfully. So, for studying the problem of contact stresses on tooth flanks, the Finite Element Method (FEM) is chosen. The Finite Element Method formulates the differential equations of balance of an elastic body. By taking into consideration the boundary conditions, the number of unknown quantities in these equations becomes smaller **Gosselin and Cloutier, 1991**.

The tooth model has been adopted from previous generation computer program, **M. Q. Abdullah and I. A. Hussain, 1999**. with means of CAD software package and solid works program, the basic input design data imported by Gleason works standards, **M. Q. Abdullah, 2007**. Fig.(2) shows three teeth of generated gear and pinion.

DEVELOPMENT OF FINITE ELEMENT MODELS

The development approach for finite element models is accomplished as follows:

- 1- Tooth surface equations of pinion and gear and portions of corresponding rim are considered for determination of the volumes of the designed bodies. Loss of accuracy introduced by CAD computer programs for the generation is avoided, **Robert F. Handschuh, 1997**.
- 2- The proposed approach does not require an assumption on the load distribution in the contact area. To get the contact area and stresses the contact algorithm of the general purpose (Ansys) is used.
- 3- F.E. models of three pairs of teeth are applied and therefore the boundary conditions are far enough from the loaded areas of the teeth.
- 4- Setting of boundary conditions is accomplished automatically and is shown in **Fig. 1**.

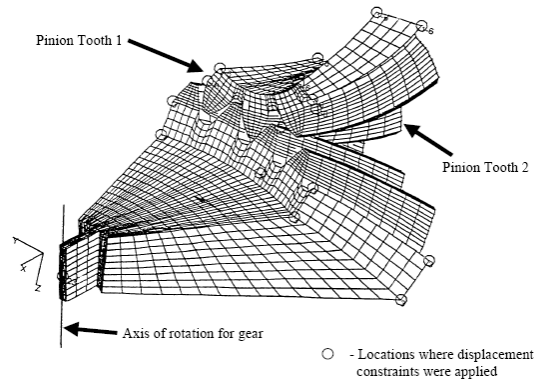


Figure 1. Boundary conditions for pinion and gear.

The following ideas are considered:

Nodes on the two sides and bottom part of the portion of the gear rim are considered as fixed.

Nodes on the two sides and bottom part of the portion of the pinion rim are considered as a rigid body.

Input torque can be expressed as the sum of applied nodal forces at radius of shaft (r_{sh}), thus

$$\mathbf{T}_1 = \sum_{i=1}^n F_i r_{sh} \quad (9)$$

Where T_1 is the input torque load, n is the total number of constrained nodes and F_i is the tangential nodal force (usually $F_i = F$, where F is a constant value). The displacement of two sides and bottom part on the pinion tooth has a unique value because a coupled equation was used to enable these surfaces to be rigid in motion.

5-The contact algorithm of the FEA computer program requires definition of contacting surfaces **,David G. and Ron L., 2003.** To define a contact pair completely, contact and target elements have to be referred to the same characteristic parameters. The element Solid 92 with 10 nodes is used as a contact surface to surface in the present analysis.

6-The select contact algorithm was the Penalty Method. The penalty method uses a contact “spring” to establish a relationship between the two contact surfaces.

NUMERICAL EXAMPLE

The finite element analysis has been performed. A three teeth model has been applied for each case of design. The element "solid 10 node 92" has been adopted to build the finite element mesh. The total number of elements is 72820 with 84614 nodes. The material steel is applied for both pinion and gear. A torque of 400 N.m has been applied to the pinion for all cases of design.

Figs.(5, 6) show the results of execution of Ansys program to evaluate contact and bending stresses numerically by choosing Von-Mises failure criterion with changing design parameters. Also **Tables (4, 5)** shows the comparison between experimental and numerical results.



Table 1. Photoelastic material properties.

Elastic Limits N/m^2	Tensile Strength N/m^2	Young's Modulus N/m^2	Poisson's Ratio
2.068427e+007	4.136854e+007	4.295434e+009	0.35

Table 2. Dimensions of gear tooth model.

Normal Module (mm)	Normal Pressure Angle (Deg)	Spiral Angle (Deg)	Face Width (mm)	Number of Pinion Teeth	Number of Gear Teeth
5	25	35	4	19	62

Table 3. Results of Calibration test.

Fringe Order, n	Load, F (N)	Stress, σ (MPa)
0	0	0
1	624.28	10.404
2	836.72	13.945
3	1024.52	17.075
4	1266.98	21.1163
5	1472.61	24.5435
6	1682.23	28.0371
7	1870.79	31.179
8	2063.82	34.397
9	2283.17	38.0528
10	2503.17	41.7226

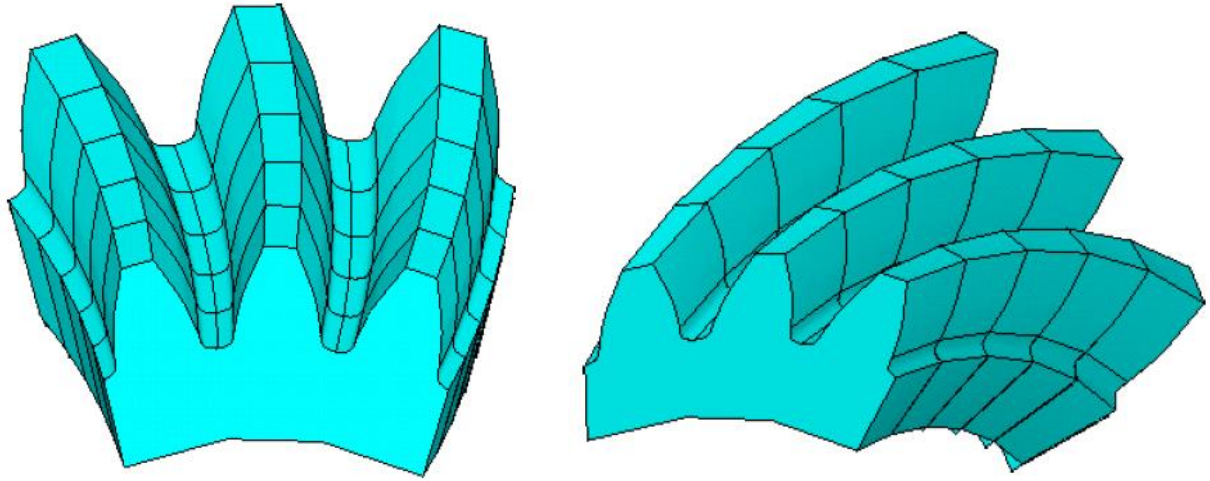


Figure 2. Three generated teeth of gear and pinion.

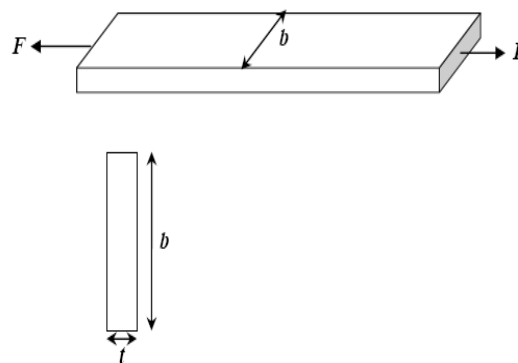


Figure 3. Schematic diagram for the tensile specimen geometry.

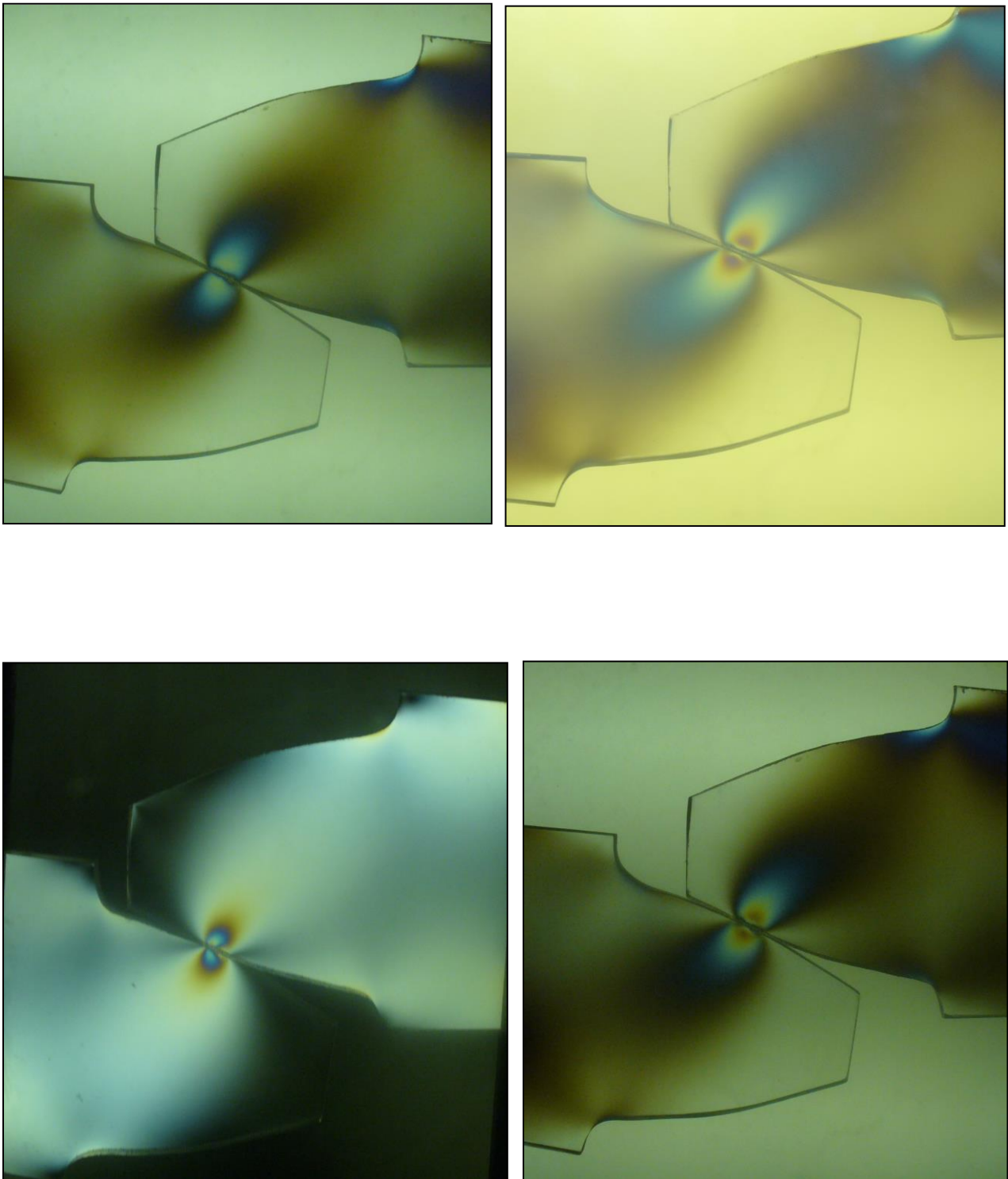
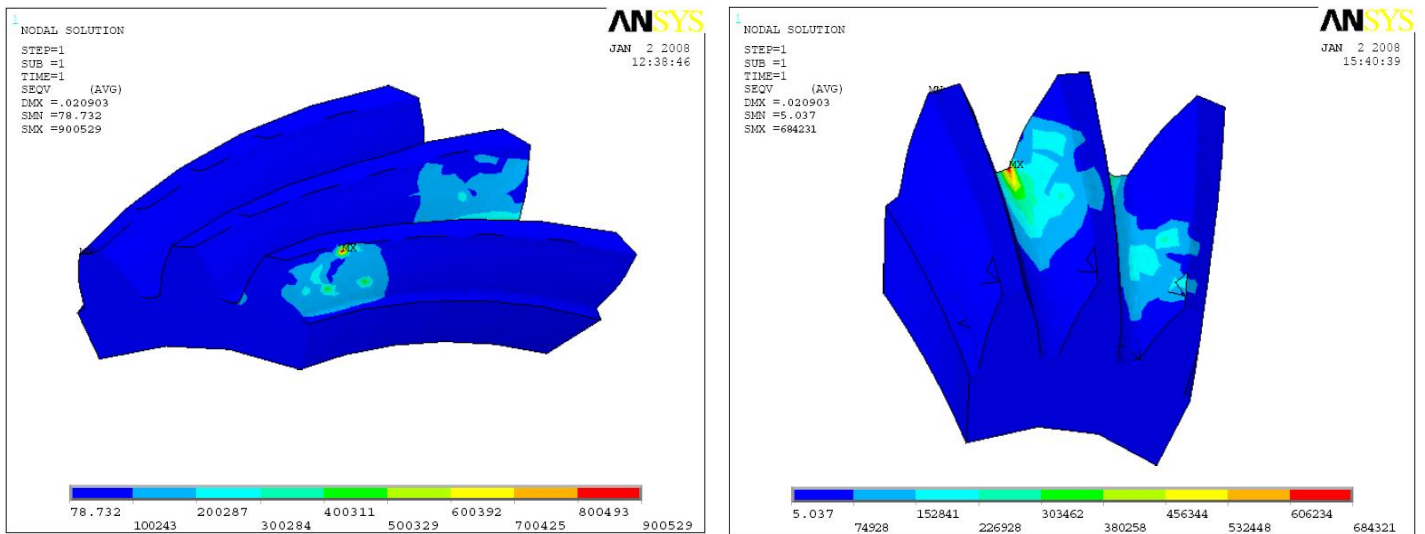
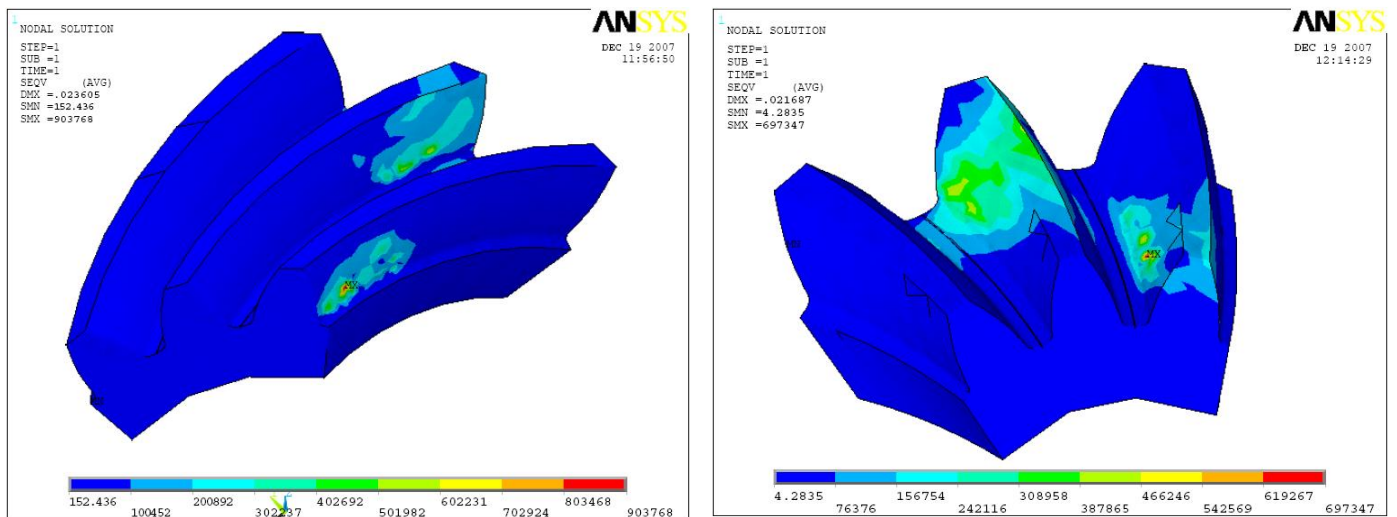


Figure 4. Results of photoelastic fringes shows gradually increasing the contact and bending stresses for both light and dark field.



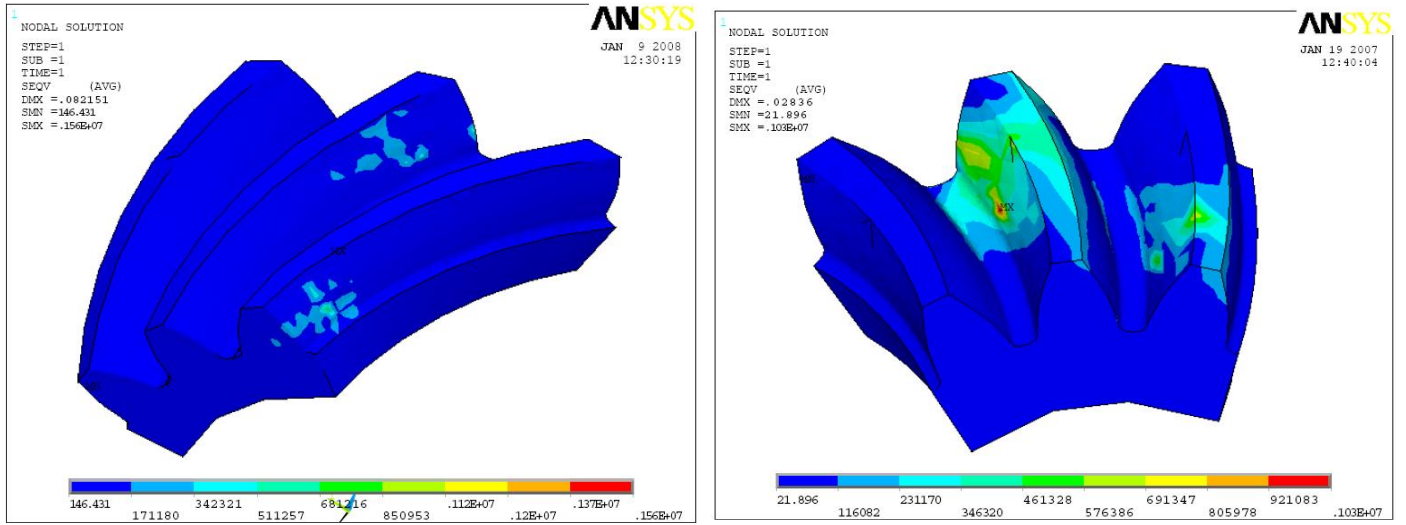
(a)



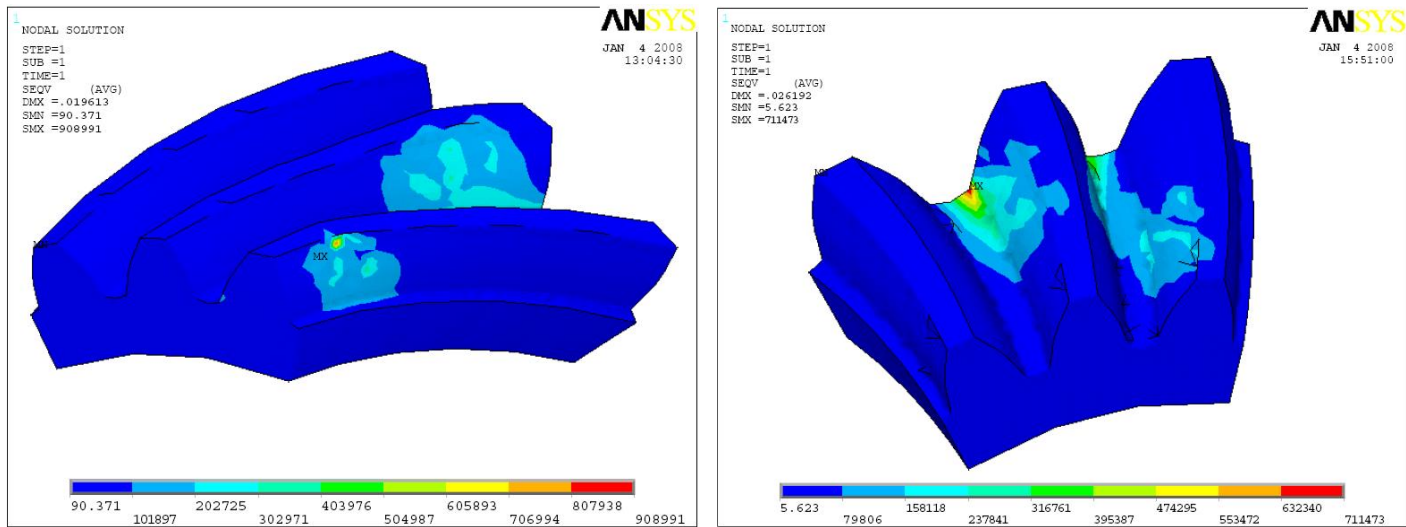
(b)

Figure 5. Von Mises contact and bending stresses with changing of spiral angle.

(a) $\beta=25.0^\circ$, (b) $\beta=35.0^\circ$



(a)



(b)

Figure 6. Von Mises contact and bending stresses with changing of Normal Module.

(a) Mn=3mm, (b) Mn=9 mm

**Table 4.** Comparison between experimental and numerical contact stresses.

	Experimental Contact Stress (Mpa)	Numerical Contact Stress (Mpa)	Percentage Error (%)
Pinion	1328.02	1372.5	3.34
Gear	1162.35	1247.3	7.308

Table 5. Comparison between experimental and numerical bending stresses.

	Experimental Bending Stress (Mpa)	Numerical Bending Stress (Mpa)	Percentage Error (%)
Pinion	288.7	248.9	15.9
Gear	242.3	221.3	9.48

CONCLUSIONS

1. Experimental and numerical analyses have been successfully conducted.
2. Automatic generation of finite element models have been developed to perform multi-tooth stress analysis for several contact points along the path of contact and obtain the contact and bending tooth stresses.
3. The investigation shows that the increasing of mean spiral angle causes increase contact stresses while the bending stresses decrease, also the increasing in the normal module leads to decrease the both contact and bending stresses, all of that indicate the improvement in the shape of transmission error function from linear to parabolic function from the point of view of minimizing transmission error which caused by misalignment.



NOMENCLATURES

A	length of major axis of contact ellipse
B	length of major axis of contact ellipse
b	width of specimen
C_p	constant
E	modulus of elasticity
F	tangential Force
f	material fringe constant
M_n	normal module
n	fringe order
T	input torque
t	thickness of specimen
r_{sh}	radius of shaft
W	applied load
β	mean spiral angle
σ_1	first principal stress
σ_2	second principal stress
ν	poisson's Ratio

REFERENCES

- David G. Lewicki, Ron L. Woods, Evaluation of low-noise, improved bearing contact spiral bevel gears, NASA TR-2970, 2003.
- Faydor L. Litvin, Alfonso Fuentes, Computerized design, Generation, Simulation of meshing and contact, and stress analysis of formate cut spiral bevel gear drives, NASA CR-525, 2003.
- Gosselin C, Cloutier L., Brousseau J., Tooth contact analysis of high conformity spiral bevel gear, NASA CR-341, 1991.
- Litvin F. L., Lee H., Generation and tooth contact analysis of spiral bevel gears with predesigned parabolic functions of transmission errors, NASA TR-C-014, 1989.
- Lelkes M., Marialigeti J., Cutting definition for kinematic optimization of spiral bevel gears, Hungary 2002.
- Mohammad Qasim Abdullah, Influence of Varying The Normal Load Position on Maximum Tensile Stresses on Unsymmetrical Gear Tooth, University of Baghdad Engineering Journal, ISSN 1726-4073, Vol.3, No.2, 1997.



- Mohammad Qasim Abdullah, Imad Ahmed Hussain, Computer Aided Graphics of Involute Gear Tooth Profile, University of Baghdad Engineering Journal, ISSN 1726-4073, Vol.5, No.1, 1999.
- Mohammad Qasim Abdullah, Machine-tool settings to provide optimal TCA of spiral bevel gear drives, University of Baghdad Engineering Journal, ISSN 1726-4073, Vol.13, No.4, 2007.
- Robert F. Handschuh , Recent advances in the analysis of spiral bevel gears, NASA ARL-TR-1316, 1997.
- Robert F. Handschuh, George D. Bibel, Comparison of experimental and analytical tooth bending stress of aerospace spiral bevel gears, NASA ARL-TR-1891, 1999.